International Journal of Heat and Technology
Vol. 42, No. 3, June, 2024, pp. 795-804
Journal homepage: http://iieta.org/journals/ijht

Thermal Conductivity Study of Plasma-Sprayed Iron-Based Coatings

Bo Zhou[1*], Wei He[2], Yile Liu[1]

[1] School of Electrical and Control Engineering, Ningxia Vocational Technical College of Industry and Commerce, Yinchuan 750021, China
[2] Sharing Intelligent Equipment Limited Company, Yinchuan 750021, China

Corresponding Author Email: zbzb.8160@163.com

https://doi.org/10.18280/ijht.420309

Received: 3 January 2024
Revised: 26 April 2024
Accepted: 8 May 2024
Available online: 27 June 2024

Keywords:
plasma spraying, iron-based coating, thermal conductivity, coupled heat transfer model, conduction boundary conditions, heat transfer coefficient, numerical simulation

ABSTRACT

Plasma spraying technology, known for its efficient surface enhancement capabilities, has been widely applied in aerospace, automotive manufacturing, and power generation. Iron-based coatings, due to their superior mechanical properties and wear resistance, have become important materials in these fields. However, under extreme working conditions such as high temperatures, high speeds, and heavy loads, the thermal conductivity of the coating directly affects its service life and stability. Therefore, studying the thermal conductivity of plasma-sprayed iron-based coatings is of great significance. Currently, research on the thermal properties of plasma-sprayed coatings primarily focuses on the surface thermal conductivity, neglecting the complex coupled heat transfer mechanisms within the coating. Moreover, existing research methods often rely on empirical formulas or simplified models, making it challenging to comprehensively reflect the thermal conductivity behavior under actual working conditions. This is especially true in high-temperature and high-pressure environments where the limitations of these methods are more pronounced. This paper establishes a coupled heat transfer model for plasma-sprayed iron-based coatings to explore their thermal conductivity under different working conditions. The study comprises three parts: first, the mathematical derivation of the coupled heat transfer model within the plasma-sprayed iron-based coating; second, the determination of conduction boundary conditions and the calculation of heat transfer coefficients; third, the simulation results of the thermal conductivity characteristics of the plasma-sprayed iron-based coating. This research not only fills the gaps in existing studies but also provides reliable theoretical support and data reference for practical engineering applications.

1. INTRODUCTION

Plasma spraying technology, as an efficient surface strengthening method, has been widely used in the field of materials engineering [1-4]. Iron-based coatings, due to their excellent mechanical properties and wear resistance, are widely used in aerospace, automotive manufacturing, power generation, and other industrial fields [5-9]. However, as the working environment becomes increasingly harsh, especially under extreme conditions such as high temperature, high speed, and heavy load, understanding the thermal conductivity of iron-based coatings becomes particularly important. This not only helps to improve the durability and stability of the coatings but also provides a theoretical basis for their optimized design in different application fields.

Studying the thermal conductivity of plasma-sprayed iron-based coatings has important practical significance. On the one hand, a thorough understanding of the internal heat conduction mechanism of the coating can help engineers better predict the performance of the coating under extreme working conditions and avoid failure caused by thermal stress [10-13]. On the other hand, by optimizing the thermal conductivity of the coating, its application efficiency can be effectively improved, the service life of the equipment can be extended, maintenance costs can be reduced, and economic benefits can be enhanced.

Although there have been many studies on the thermal properties of plasma-sprayed coatings, most of them are limited to the thermal conductivity of the coating surface and ignore the complex coupled heat transfer mechanism inside the coating [14, 15]. In addition, the existing research methods are mostly empirical formulas or simplified models, which are difficult to comprehensively reflect the thermal conductivity behavior under actual working conditions [16-19]. Especially in high-temperature and high-pressure environments, the limitations of these methods are more obvious, and they lack accurate calculations of heat transfer boundary conditions and heat transfer coefficients, resulting in limited accuracy and reliability of the research results [20-22].

This paper aims to explore the thermal conductivity of plasma-sprayed iron-based coatings under different working conditions by establishing a coupled heat transfer model. The main research content includes three parts: first, the mathematical derivation of the coupled heat transfer model within the plasma-sprayed iron-based coating, establishing an

accurate mathematical model through theoretical analysis; second, the determination of conduction boundary conditions and the calculation of heat transfer coefficients, ensuring the accuracy and applicability of the model; third, the simulation results of the thermal conductivity characteristics of the plasma-sprayed iron-based coating, verifying the effectiveness of the model through numerical simulation methods. Through these studies, not only can the gaps in existing research be filled, but also reliable theoretical support and data references can be provided for practical engineering applications, which has important academic value and engineering application prospects.

2. MATHEMATICAL DERIVATION OF THE COUPLED HEAT TRANSFER MODEL FOR PLASMA-SPRAYED IRON-BASED COATINGS

In the industrial sodium production process, the cathode tube is one of the critical components, enduring long-term exposure to high temperatures and strong corrosive environments. Therefore, the cathode tube is prone to thermal deformation and corrosion failure, leading to a shortened service life. Once a local defect appears in the cathode tube, it usually results in the scrapping of the entire component, causing significant waste and substantially increasing production costs. Thus, effectively repairing the defects on the inner wall of the cathode tube and extending its service life have become urgent technical challenges in the field of industrial sodium production. This paper explores the application of plasma spraying technology in the repair of industrial sodium cathode tubes, specifically studying the thermal conductivity of plasma-sprayed iron-based coatings. Plasma spraying is an advanced surface modification technology that melts materials at high temperatures and sprays them onto the substrate surface, forming a dense and strongly adherent coating. Compared to traditional repair methods, it has a series of significant advantages. Specifically, plasma spraying technology can quickly form a uniform iron-based coating on the inner wall of the cathode tube, effectively covering and filling surface defects, restoring its integrity and function. At the same time, iron-based coatings have good thermal conductivity, which can effectively alleviate the thermal stress of the cathode tube in high-temperature environments and reduce the occurrence of thermal deformation. Plasma spraying technology can also form a highly adherent coating on the inner wall of the cathode tube, ensuring that the coating is not easy to peel off in high-temperature and corrosive environments. Figure 1 shows a schematic diagram of the plasma-sprayed iron-based coating.

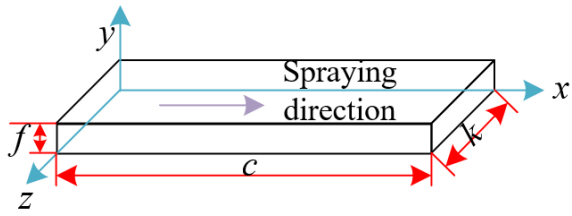

Figure 1. Schematic diagram of plasma-sprayed iron-based coating

The study of the thermal conductivity of plasma-sprayed iron-based coatings is a complex process involving the microstructural characteristics, physical properties, and thermal radiation properties of the coating. The mathematical modeling of coupled heat radiation and heat conduction plays a crucial role in this study, providing an in-depth understanding and quantitative analysis of the internal heat transfer mechanism of the coating.

Table 1. Physical parameters of plasma-sprayed iron-based coating

Temperature ℃	Density $Kg.m^{-3}$	Specific Heat Capacity $J.Kg^{-1}.℃^{-1}$	Thermal Conductivity $W.m^{-1}.℃^{-1}$	Thermal Expansion Coefficient $10^{-6}.℃^{-1}$	Elastic Modulus GPa	Poisson's Ratio
20	6910	520	9.5	15	168	0.25
200		820	9.5	16	128	0.26
400		890	9.6	17.2	115	0.27
600		1110	10.2	17.6	83	0.3
800		1110	11.2	18	47	0.31
1000		1350	14	18.4	9.3	0.37
1070		1350	21	18.6	1	0.37
1100		1350	21	19.2	1	0.37

Due to the rapid cooling and solidification of the metal particles melted at high temperatures during the spraying process on the substrate surface, the coating often presents a layered structure and may contain pores and microcracks. These microstructural characteristics significantly affect the thermal conductivity because they change the thermal conduction paths and heat dissipation efficiency. Moreover, the physical properties of iron-based coatings, such as thermal conductivity and specific heat capacity, are key parameters affecting their thermal conductivity. Since the thermal conductivity of iron-based coatings may change with temperature, it is necessary to accurately describe the temperature dependence of these physical properties in steady-state heat conduction problems. Additionally, the thermal radiation properties of iron-based coatings cannot be ignored in high-temperature environments. Thermal radiation not only affects the heat flow exchange on the surface of the coating but also may transfer heat within the coating through radiation. Therefore, establishing an accurate mathematical model can help us understand and quantify the impact of the microstructural characteristics of plasma-sprayed iron-based coatings on thermal conductivity while systematically incorporating their physical properties into the heat conduction equations, thereby precisely predicting the internal temperature distribution of the coating.

Specifically, this paper derives the relationship between spectral radiance $H_{\lambda j}(c)$ and temperature $S(c)$, the relationship between the surface temperature $S(0)$ and the total heat flux w_{TOT} of the coating, and the relationship between temperature $S(c)$ and w_{TOT}, $S(0)$, $H_{\lambda j}(c)$. The mathematical model can systematically integrate these influencing factors, providing a comprehensive description of coupled heat conduction and

thermal radiation heat transfer. This model can not only explain current experimental data but also predict the thermal conductivity behavior of the coating under different conditions, providing theoretical support for optimizing the preparation process and improving performance.

The relationship between spectral radiance $H_{\Lambda j}(c)$ and temperature $S(c)$ is fundamental to understanding the thermal radiation behavior inside the coating. According to Planck's law, the radiance at each wavelength depends on temperature. Therefore, the temperature distribution $S(c)$ within the coating will directly affect the spectral radiance $H_{\Lambda j}(c)$ at each coordinate position c. Due to the presence of pores and cracks in the microstructure of plasma-sprayed iron-based coatings, these inhomogeneities will cause scattering and absorption of radiation, thereby affecting the radiation transmission path. By incorporating these microstructural characteristics into the model, the transfer process of thermal radiation within the coating can be more accurately described. Assuming that the refractive index of the bottom layer (V-th layer) of the plasma-sprayed iron-based coating is represented by $v^{(V)}$, the function mapping coordinate c to the corresponding layer number is represented by $m(c)$, the Stefan-Boltzmann constant in blackbody radiation is represented by δ, the ratio of the radiant energy contained in the wavelength band Λ_j to the total radiant energy in blackbody radiation at temperature S is represented by $D(\Lambda_j,S)$, the total thickness of the plasma-sprayed iron-based coating is represented by f, and the thickness of the u-th layer of the plasma-sprayed iron-based coating is represented by f_u, the following differential equation is given for the spectral radiance $H_{\Lambda j}(c)$ in the wavelength band Λ_j at coordinate zc:

$$\frac{d^2 H_{\Lambda_j}(c)}{dc^2} + 3\overline{j_{\Lambda_j}^{(m(c))}}^2 \left(\overline{\Psi_{\Lambda_j}^{(m(c))}} - 1 \right) \tag{1}$$

$$\begin{aligned} &\left[H_{\Lambda_j}(c) - 4v^{(m(c))^2} \delta D\left(\Lambda_j, S(c)\right) S(c)^4 \right] = 0 \\ &H_{\Lambda_j}(c) = \int_{\eta=\eta_{j-1}}^{\eta_j} H_\eta(c)\, f\eta \end{aligned} \tag{2}$$

The corresponding boundary conditions are as follows:

$$\begin{aligned} &c = 0: \\ &H_{\Lambda_j}(0) = \frac{2(1+\vartheta_u)}{3\overline{j_{\Lambda_k}^{(m(z))}}(1-\vartheta_u)} \frac{H_{\Lambda_j}(c)}{fc}\Big|_{z=0} \\ &+4\frac{1-\vartheta_p}{1-\vartheta_u} \delta D\left(\Lambda_j, S_{GA}\right) S_{GA}^4 \end{aligned} \tag{3}$$

$$\begin{aligned} &c = f: \\ &H_{\Lambda_j}(f) = \frac{2}{3\overline{j_{\Lambda_j}^{(m(c))}}} \left(\frac{2}{\in_l} - 1 \right) \frac{H_{\Lambda_j}(c)}{fc}\Big|_{c=f} \\ &+4v^{(V)^2} \delta D\left(\Lambda_j, Sf\right) Sf^4 \end{aligned} \tag{4}$$

The reflectivity on the outer and inner sides of the coating surface is represented by ϑ_p and ϑ_u, respectively, and their calculation formulas are as follows:

$$\begin{aligned} \vartheta_p = &\frac{1}{2} + \frac{(3v+1)(v-1)}{6(v+1)^2} + \frac{v^2(v^2-1)}{(v^2+1)^3} LN\left(\frac{v-1}{v+1}\right) \\ &- \frac{2v^3(v^2+2v-1)}{(v^2+1)(v^4-1)} + \frac{8v^4(v^4+1)}{(v^2+1)(v^4-1)^2} LN(v) \end{aligned} \tag{5}$$

$$\vartheta_u = 1 - \frac{1-\vartheta_p}{v^2} \tag{6}$$

The relationship between the surface temperature $S(0)$ and the total heat flux w_{TOT} is the key to defining the overall heat transfer performance of the coating. According to Fourier's law, the heat flux density in the conduction process is proportional to the temperature gradient, and the surface temperature $S(0)$ is the boundary condition of this temperature gradient. The thermal conductivity of plasma-sprayed iron-based coatings may vary with temperature and microstructure, so it is necessary to determine the effective thermal conductivity of the coating through experimental data or theoretical analysis. Combining this information, the relationship between the total heat flux w_{TOT} and the surface temperature $S(0)$ can be established to describe the heat flow conduction behavior of the coating under steady-state conditions. Specifically, suppose the temperature of the substrate below the plasma-sprayed iron-based coating in actual applications is F. This paper first constructs the heat balance equations at the two boundaries c=0 and c=F+f of the coating-substrate, further deriving the relationship between $S(0)$ and w_{TOT}. Suppose the convective heat transfer coefficients between the upper surface of the plasma-sprayed iron-based coating and the solution, and the lower surface of the substrate and the external airflow are represented by g_1 and g_2, the thermal conductivity of the plasma-sprayed iron-based coating is represented by j_u, the thermal conductivity of the substrate is represented by j_y, and the thermodynamic temperatures of the solution above the coating and the external airflow of the substrate are represented by S_{GA} and S_{CO} respectively, then we have:

$$X \begin{bmatrix} w_{TOT} \\ S(0) \end{bmatrix} = Y \tag{7}$$

The expressions of matrices X and Y are:

$$X = \begin{bmatrix} 1 & -g_1 \\ \dfrac{1}{g_2} + \dfrac{D}{j_y} + \sum_{u=0}^{V} \dfrac{f_u}{j_u} & -1 \end{bmatrix} \tag{8}$$

$$Y = \begin{bmatrix} g_1 S_{GA} + 2\dfrac{1-\vartheta p}{1+\vartheta_u} \sum_{k=1}^{J} \vartheta S_{GA}^4 D\left(\Lambda_k, S_{GA}\right) \\ -\dfrac{1}{2}\dfrac{1-\vartheta u}{1+\vartheta u} \sum_{k=1}^{J} H_{\Lambda_k}(0) \\ -S_{CO} + \sum_{u=1}^{V} \sum_{k=1}^{J} \dfrac{H_{\Lambda_k}\left(\sum_{j=1}^{u-1} f_j\right) - H_{\Lambda_k} \sum_{j=1}^{u} f_j}{3\overline{j^{(u)}} j_u} \end{bmatrix} \tag{9}$$

The relationship between temperature $S(c)$ and w_{TOT}, $S(0)$, $H_{\Lambda j}(c)$ is the core of the entire mathematical model. By solving

the heat conduction equation and the radiation transfer equation, the internal temperature distribution $S(c)$ of the coating can be expressed as a function of the total heat flux, surface temperature, and spectral radiance. The coupled heat conduction and thermal radiation heat transfer process of plasma-sprayed iron-based coatings needs to consider the thermal physical parameters of the material, such as the temperature dependence of the thermal conductivity and specific heat capacity, as well as radiation characteristic parameters such as the radiation absorption coefficient and scattering coefficient. These parameters can be obtained through experimental measurements or numerical simulations and comprehensively processed in the model to accurately describe the complex heat transfer mechanism within the coating.

Under the known conditions of q_{tot}, $T(0)$, and $G_\lambda(z)$, the temperature distribution $S(c)$ within the plasma-sprayed iron-based coating can be calculated by the following formula:

$$S(c)=S(0)-\sum_{u=1}^{m(c)-1}\frac{w_{TOT}\,f_u}{j_u}-\frac{w_{TOT}\left(c-\sum_{j=1}^{m(c)}f_j\right)}{j_{m(c)}} \tag{10}$$

Based on Fourier's law of heat conduction, the temperature distribution $S(c)$ within the substrate can be calculated based on the thermal conductivity j_y of the substrate. Furthermore, the temperature distribution within the plasma-sprayed iron-based coating-substrate system can be obtained. Figure 2 shows the temperature curves in different directions of the plasma-sprayed iron-based coating-substrate system.

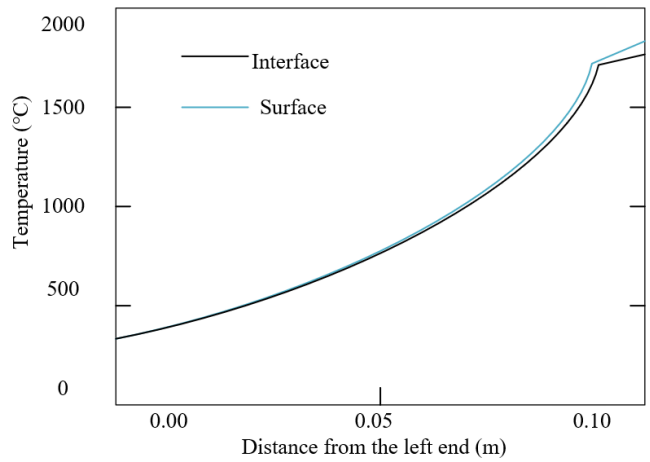

1) Centerline direction

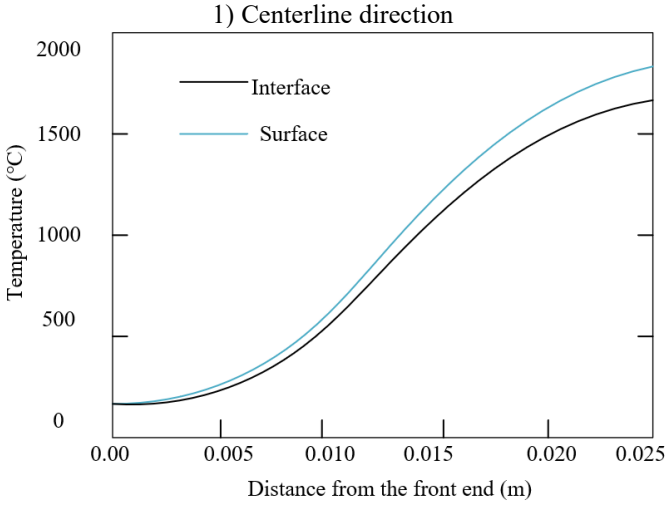

2) Width direction

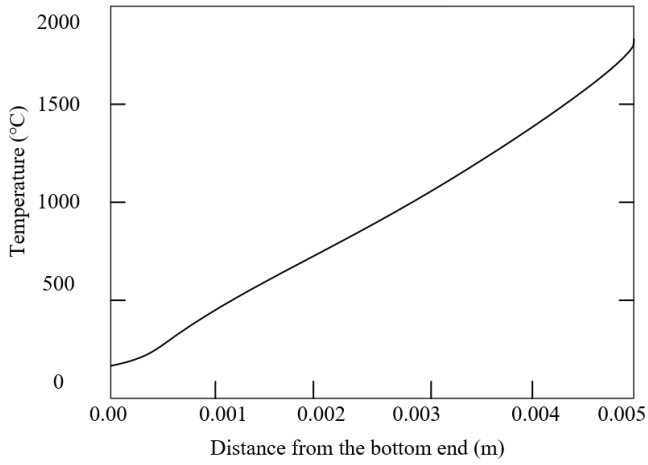

3) Thickness direction

Figure 2. Temperature curves in different directions of the plasma-sprayed iron-based coating-substrate system °C

To achieve the coupled heat transfer solution within the plasma-sprayed iron-based coating, this paper introduces an iterative method. The core idea of this method is to gradually approach the temperature distribution within the coating to accurately describe the thermal conductivity of the coating. This method ignores the effect of thermal radiation and only considers the heat conduction process under convective boundary conditions on both sides to obtain the initial temperature distribution. After obtaining the initial temperature distribution $S(c)^{(0)}$, the next step is to calculate the upper surface temperature $S(0)^{(0)}$ of the coating, the total heat flux $w^{(0)}{}_{TOT}$, and the radiation amount $H_{\lambda k}(c)^{(0)}$ in each wavelength band. These initial values are determined by the preliminary solution of the heat conduction equation and the radiation transfer equation, reflecting the heat transfer state without considering the effect of radiation. Subsequently, these initial values are substituted into the equations that comprehensively consider the coupled effect of thermal radiation and heat conduction to recalculate the temperature distribution $S(c)^{(1)}$ within the coating. Through such iterative processes, using the temperature distribution obtained from the previous calculation and the related radiation and heat flux parameters each time, the temperature distribution within the coating is updated. Each iteration gradually approaches the temperature field in the actual situation until the temperature distribution $S(c)$ converges, meaning that the temperature change between two iterations tends to zero. When the temperature distribution converges, it indicates that a stable solution has been found, and the coupled heat transfer problem is solved.

3. DETERMINATION OF CONDUCTIVE BOUNDARY CONDITIONS FOR PLASMA-SPRAYED IRON-BASED COATINGS

When conducting thermal conductivity simulation analysis of plasma-sprayed iron-based coatings, especially in considering the application scenario of repairing the inner wall of industrial sodium cathode tubes, determining the conductive boundary conditions is a crucial step. These boundary conditions directly affect the accuracy of the simulation results and the effectiveness of practical applications. Based on the study of the thermal conductivity of

plasma-sprayed iron-based coatings and considering the chemical composition of the materials and the application environment, this paper details the basic principles of constructing conductive boundary conditions.

Firstly, it is necessary to clarify the working environment of the industrial sodium cathode tube and its thermal conduction characteristics. The inner wall is in direct contact with high-temperature sodium liquid, which means that the primary heat transfer mode for the inner wall is convective heat transfer. The temperature and convective heat transfer coefficient of the sodium liquid are key parameters. Meanwhile, the outer wall is usually in contact with ambient air, and the convective heat transfer coefficient and ambient temperature of the air also need to be determined. Besides convective heat transfer, thermal radiation is another important factor that needs to be considered. Due to the high temperature of the coating, radiative heat flux cannot be ignored. The Stefan-Boltzmann law is used to describe radiative heat flux, and the emissivity of the coating and the Stefan-Boltzmann constant are key parameters for describing radiative heat flux. In terms of chemical composition, the coating mainly consists of iron and other elements (such as C, Cr, Si, Ni, Mn), which affect the thermal conductivity and radiation properties of the coating. Referencing the chemical composition of the coating (50 kg): C greater than 0.2%, Cr less than 17.5%, Si less than 0.75%, Ni less than 0.6%, Mn less than 1%, Fe balance, the proportions of these components directly impact the thermal physical parameters of the coating. Therefore, when constructing boundary conditions, it is necessary to comprehensively consider the impact of these components on the thermal conductivity of the material.

In the study of the thermal conductivity of plasma-sprayed iron-based coatings, constructing a three-dimensional transient heat conduction model and its corresponding boundary conditions is a core step. The transient behavior of heat conduction refers to the change of temperature with time and space, which needs to be described by a mathematical model. In this process, determining the heat exchange mode of the coating surface and its environment is key. In the three-dimensional transient heat conduction process, this paper uses the function $\theta=\theta(a,s)$ to characterize the temperature field, which is a function of space $a=\{a,b,c)^T$ and time s within the coating domain Ψ. Assume the thermal conductivity of the coating along the a, b, and c directions is represented by j_a, j_b, and j_c, respectively, the specific heat capacity of the coating is represented by z, the density of the coating is represented by ϑ, and the heat source density within the domain is represented by W, $W=W(a,s)$. The temperature field satisfies the partial differential equation shown below:

$$\begin{aligned}&\frac{\partial}{\partial a}\left(j_a\frac{\partial\theta}{\partial a}\right)+\frac{\partial}{\partial b}\left(j_b\frac{\partial\theta}{\partial b}\right)+\frac{\partial}{\partial c}\left(j_c\frac{\partial\theta}{\partial c}\right)\\&=\rho z\frac{\partial\theta}{\partial s}-\vartheta W\left(a\in\Psi\right)\end{aligned}\tag{11}$$

Boundary conditions include the following three types:

First type: The case of given boundary temperature $\theta=\bar{\theta}$ ($a\in\Delta_1$) applies when the temperature of the boundary of the plasma-sprayed iron-based coating is explicitly known and does not change. In some applications, part of the coating may be in direct contact with a part or medium with a constant temperature, in which case we can directly set this temperature value in the boundary condition. Assuming that the entire boundary of the coating domain Ψ is represented by Δ, $\Delta=\partial\Psi=\Delta_1+\Delta_2+\Delta_3$, the expression is:

$$\theta=\bar{\theta}\left(a\in\Delta_1\right)\tag{12}$$

Second type: The case of given boundary heat flux density applies when the heat flow on the boundary of the plasma-sprayed iron-based coating is known. Heat flux density refers to the amount of heat flow per unit area, which usually occurs in the case of a known heat source or cooling device. If there is a known heat source continuously supplying heat to the coating surface, the heat flux density can be used as a boundary condition. Assuming that the unit outward normal vector on the boundary of the plasma-sprayed iron-based coating is represented by v, $v=\{v_a(\Delta),v_b(v),v_c(\Delta)\}$, and the boundary heat flux density of Δ_2 is w, $w=w(\Delta_2,s)$, the expression is:

$$j_a\frac{\partial\theta}{\partial a}v_a+j_b\frac{\partial\theta}{\partial b}v_b+j_c\frac{\partial\theta}{\partial c}v_c=w\left(a\in\Delta_2\right)\tag{13}$$

Third type: The case of heat exchange with a fluid at a certain temperature applies when the boundary of the plasma-sprayed iron-based coating exchanges heat with the environment through convection and radiation. In practical applications, a surface of the coating may be exposed to air or in contact with cooling liquid, in which case the boundary condition needs to consider not only the temperature change but also the heat transfer coefficient, ambient temperature, and radiation effects. Assuming that the convective heat transfer coefficient is represented by g, and the cold source temperature is represented by θ_x, $\theta_x=\theta_x(\Delta_3,s)$, the expression is:

$$j_a\frac{\partial\theta}{\partial a}v_a+j_b\frac{\partial\theta}{\partial b}v_b+j_c\frac{\partial\theta}{\partial c}v_c=g=\left(\theta_x-\theta\right)\left(a\in\Delta_3\right)\tag{14}$$

By combining these three types of boundary conditions, it is possible to simulate in detail the thermal conduction behavior of the coating in actual working environments, helping to predict the temperature distribution and thermal stress of the coating under different operating conditions, thereby optimizing material selection and spraying processes, and improving the performance and durability of the coating. Specifically, in the application of industrial sodium cathode tubes, the inner wall requires the application of given boundary temperature conditions, while the outer wall needs to consider the heat exchange with ambient air. This comprehensive method of constructing boundary conditions ensures the accuracy and practicality of the thermal conduction model.

The study of the thermal conductivity of plasma-sprayed iron-based coatings aims to evaluate and optimize the thermal conduction behavior of the coating in high-temperature environments, with the core being the accurate calculation of the heat transfer coefficient. The calculation of the heat transfer coefficient involves multiple aspects, including the microstructural characteristics, physical properties, and thermal radiation properties of the coating. In terms of microstructural characteristics, the plasma spraying process usually forms microscopic pores and cracks within the coating, which can reduce the overall thermal conductivity of the coating. Specifically, pores in the coating increase thermal resistance, while cracks may make the thermal conduction

path discontinuous, thereby reducing thermal conductivity efficiency. In terms of physical properties, iron (Fe) in the iron-based coating mainly provides the structural strength and thermal conductivity of the matrix, while the presence of elements such as carbon (C) and chromium (Cr) increases the hardness and wear resistance of the coating but may also affect its thermal conductivity. For example, a high content of chromium (Cr) forms hard carbide phases, which, although improving wear resistance, typically have lower thermal conductivity than the pure iron matrix, thereby reducing the overall thermal conductivity of the coating. In terms of thermal radiation properties, the surface roughness of the iron-based coating and the presence of an oxide layer can change its radiation properties. Generally, coatings with higher surface roughness have higher radiation absorption rates, while oxide layers increase the radiation emissivity of the coating. Therefore, when calculating the heat transfer coefficient, it is necessary to comprehensively consider the thermal radiation properties of the coating, especially its radiation behavior in high-temperature environments. Assuming that the heat transfer per unit area is represented by w, the convective heat transfer coefficient is represented by g, and the average temperature difference between the fluid and the unit heat transfer surface is represented by Δs, the heat transfer coefficient can be calculated using Newton's cooling formula:

$$w = g\Delta s \tag{15}$$

Assuming the thermal conductivity of the fluid involved in heat transfer is represented by η, the Prandtl number of the fluid is represented by Pr, the characteristic length of the heat transfer component is represented by m, and the Reynolds number of the fluid flow is represented by Re. When $Re<5*10^5$ and $Pr>=0.6$, the convective heat transfer coefficient can be calculated by the following formula:

$$g_{m1} = \frac{0.644\eta}{m}\mathrm{Re}_1^{\frac{1}{2}}\mathrm{Pr}^{\frac{1}{2}} \tag{16}$$

When $Re<5*10^5$ and $0.6<Pr<60$, the convective heat transfer coefficient can be calculated by the following formula:

$$g_{m2} = 0.037\frac{\eta}{m}\left(\mathrm{Re}_m^{\frac{4}{5}} - 871\right)\mathrm{Pr}^{\frac{1}{3}} \tag{17}$$

The thermal conduction model for plasma-sprayed iron-based coatings includes specific parameters such as the geometric dimensions and material properties of the substrate, bonding layer, and wear-resistant coating. Assume the substrate material is nickel-based high-temperature alloy GH4169, with dimensions of 30mm×20mm and a thickness of 5mm. The bonding layer and wear-resistant coating have dimensions of 30mm×20mm and a thickness of 0.1mm. The material of the wear-resistant component is cobalt-based high-temperature alloy GH605, and the wear-resistant coating material is plasma-sprayed iron-based coating, with the chemical composition as follows: C greater than 0.2, Cr less than 17.5, Si less than 0.75, Ni less than 0.6, Mn less than 1, Fe balance.

In the setup of boundary conditions, all surfaces except the bottom contact surface of the sample are treated as convective heat transfer surfaces, and appropriate convective heat transfer coefficients are applied to these surfaces. This means that during the calculation process, the surfaces of the coating, bonding layer, and substrate will exchange heat with the environment, simulating the heat flow conditions in the actual working environment. The selection of the convective heat transfer coefficient should be based on the actual heat dissipation capacity of the plasma-sprayed iron-based coating and its surface characteristics. The microstructure of the coating, such as pores and cracks, will affect its overall heat dissipation efficiency, so these factors need to be considered when setting the convective heat transfer coefficient. Additionally, considering the thermal expansion properties of the coating at high temperatures, the thermal expansion effect is included in the model through thermal-structural coupled analysis. This process can simulate the stress and deformation of the coating under thermal loads, reflecting its thermal conduction performance under actual working conditions. The microstructure of the plasma-sprayed coating may lead to localized stress concentration, affecting the overall thermal conduction effect.

When studying the transient thermal conduction performance of plasma-sprayed iron-based coatings, it is assumed that the wear-resistant component always remains perpendicular to the coating surface and uniformly contacts the bottom, ensuring the uniformity of load distribution. We assume that the wear-resistant coating, bonding layer, and substrate materials are isotropic and free of defects and pores, simplifying the model to focus on the thermal conduction properties of the materials themselves. For the load, five different load values are selected: 5N, 8N, 10N, 15N, and 20N. The ambient temperature is set to four conditions: room temperature, 200°C, 400°C, and 600°C.

4. SIMULATION RESULTS OF THERMAL CONDUCTIVITY CHARACTERISTICS OF PLASMA-SPRAYED IRON-BASED COATINGS

Table 2. Calculation results of convective heat transfer coefficient g_{m1} ($W/(m^2.K)$)

Temperature (℃) / Speed(*cm/ min*)	20	200	400	600
500	9.78	9.65	9.21	9.12
1000	12.35	12.22	12.41	12.35
2000	19.5	19.56	19.52	17.56
3000	23.14	23.21	22.31	21.65
4000	27.56	27.52	26.59	25.69

Table 3. Calculation results of convective heat transfer coefficient g_{m2} ($W/(m^2.K)$)

Temperature (℃) / Speed (*cm/ min*)	20	200	400	600
500	41.26	41.26	41.23	38.64
1000	58.96	57.56	56.32	54.87
2000	82.31	81.32	81.24	79.23
3000	101.56	81.25	99.58	96.31
4000	118.36	101.26	113.26	111.25

From the data in Tables 2 and 3, we can observe the variations in convective heat transfer coefficients under different temperature and speed conditions. Table 2 shows the calculation results of the convective heat transfer coefficient g_{m1}. As the speed increases, the convective heat transfer coefficient gradually increases, but the temperature has a small

effect on the heat transfer coefficient, with little variation. Specifically, when the speed increases from 500 cm/min to 4000 cm/min, the convective heat transfer coefficient increases from 9.78 W/(m².K) to 27.56 W/(m².K) at 20°C, and from 9.12 W/(m².K) to 25.69 W/(m².K) at 600°C. Table 3 shows the calculation results of the convective heat transfer coefficient g_{m2}. As the speed increases, the convective heat transfer coefficient significantly increases, and the temperature has a certain effect on the heat transfer coefficient. At 20°C, the convective heat transfer coefficient increases from 41.26 W/(m².K) to 118.36 W/(m².K), and at 600°C, it increases from 38.64 W/(m².K) to 111.25 W/(m².K). Through the analysis of the experimental data, several important conclusions can be drawn. First, the effect of speed on the convective heat transfer coefficient is significant; higher speeds significantly improve heat transfer efficiency, which is validated in both sets of data. Second, the temperature has a smaller effect on g_{m1} but a more significant effect on g_{m2}, which may be due to the different heat transfer mechanisms of different models or materials at high temperatures. Overall, as the speed increases, the convective heat transfer coefficient increases significantly, indicating that in practical applications, increasing fluid speed can effectively enhance the heat transfer performance of the coating.

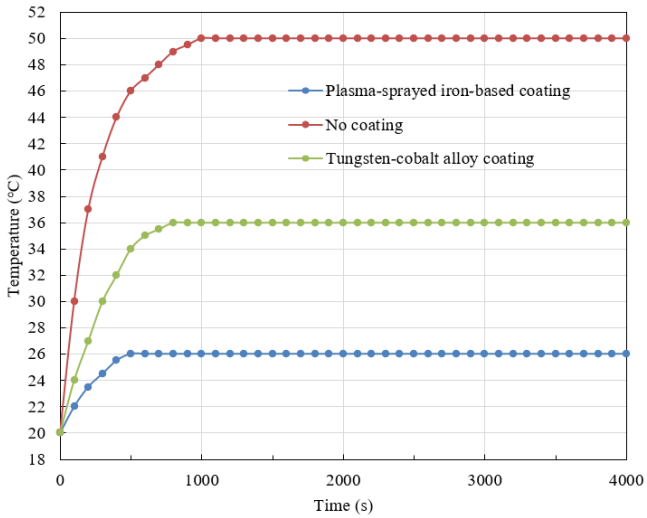

Figure 3. Temperature variation of different coatings at room temperature

Figure 3 shows the temperature data of different coatings over time at room temperature. At time zero, the initial temperature of all coatings and the non-coated material is 20°C. As time progresses, the temperature gradually rises. The temperature of the plasma-sprayed iron-based coating changes more slowly, rising to 22°C at 1000 seconds, 23.5°C at 2000 seconds, and finally stabilizing at 26°C after 3000 seconds. The temperature of the non-coated material rises faster, reaching 30°C at 1000 seconds, 37°C at 2000 seconds, and rapidly rising to 50°C after 3000 seconds, remaining constant. The temperature variation of the tungsten-cobalt alloy coating is between the plasma-sprayed iron-based coating and the non-coated material, being 24°C at 1000 seconds, 27°C at 2000 seconds, and stabilizing at 36°C after 3000 seconds. By analyzing the temperature variation data over time, several important conclusions can be drawn. The plasma-sprayed iron-based coating exhibits a significant thermal buffering effect during heat transfer, effectively slowing the temperature rise and ultimately stabilizing at 26°C, indicating its excellent thermal insulation performance. The non-coated material's temperature rises the fastest, with a final temperature of 50°C, indicating that the non-coated material conducts heat the most rapidly, lacking effective thermal protection. The tungsten-cobalt alloy coating's temperature rise rate and stable temperature are between the plasma-sprayed iron-based coating and the non-coated material, indicating that it has a certain thermal protection effect, but not as significant as the plasma-sprayed iron-based coating.

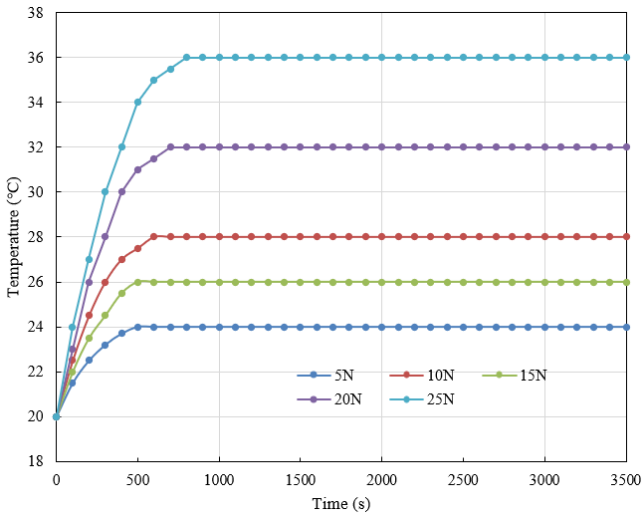

Figure 4. Surface temperature variation of plasma-sprayed iron-based coating with load

Figure 4 shows the surface temperature data of plasma-sprayed iron-based coatings under different load conditions over time. Initially, the temperature under all loads is 20°C. As time increases, the temperature variation trend under different loads gradually appears. For a 5N load, the temperature rises to 21.5°C at 500 seconds, 22.5°C at 1000 seconds, and stabilizes at 24°C after 1500 seconds. Under a 10N load, the temperature changes faster, reaching 22.5°C at 500 seconds, 24.5°C at 1000 seconds, and stabilizing at 28°C after 1500 seconds. The temperature variation under a 15N load is similar to that under a 5N load but slightly higher, with temperatures of 22°C at 500 seconds, 23.5°C at 1000 seconds, and stabilizing at 26°C after 1500 seconds. Under a 20N load, the temperature rise is more significant, reaching 23°C at 500 seconds, 26°C at 1000 seconds, and stabilizing at 32°C after 1500 seconds. Under the maximum load of 25N, the temperature rises to 24°C at 500 seconds, 27°C at 1000 seconds, and stabilizes at 36°C after 1500 seconds. The data analysis shows that the load significantly impacts the surface temperature of the plasma-sprayed iron-based coating. As the load increases, the surface temperature rises faster and eventually stabilizes at a higher temperature. Specifically, lower loads stabilize the temperature at 24°C and 26°C, while higher loads stabilize the temperature at 32°C and 36°C. This result indicates that an increase in load leads to enhanced internal heat conduction of the coating, accelerating the temperature rise and reaching a higher stable temperature.

Figure 5 shows the surface temperature and stress data of plasma-sprayed iron-based coatings under extremely low maximum stress conditions over time. Initially, the temperature is 20°C, and the stress is 4 MPa. As time progresses, both temperature and stress gradually increase. At

1000 seconds, the temperature rises to 22.8°C, and the stress is 44 MPa; at 2000 seconds, the temperature reaches 24.8°C, and the stress is 60 MPa; at 3000 seconds, the temperature is 26.4°C, and the stress is 78 MPa; at 4000 seconds, the temperature rises to 27.4°C, and the stress is 84 MPa. Thereafter, the growth rate of temperature and stress slows down, with the temperature stabilizing at 28.4°C and the stress remaining constant at 94 MPa. The data analysis shows a significant correlation between surface temperature and stress over time under extremely low maximum stress conditions. The temperature rises rapidly initially and stabilizes at 28.4°C, indicating that the coating material has good thermal stability and thermal buffering capacity. Regarding stress, the stress increases rapidly from the initial 4 MPa to 94 MPa and remains stable, indicating that the coating material can withstand high stress without significant deformation or damage under extremely low maximum stress conditions.

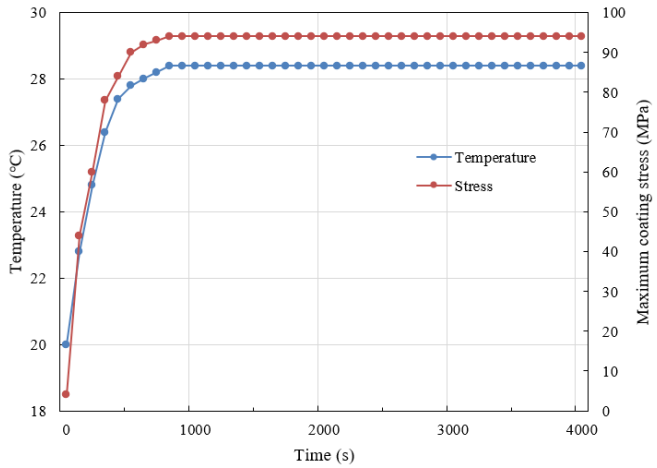

Figure 5. Surface temperature and extremely low maximum stress of plasma-sprayed iron-based coating over time

Figure 6 shows the temperature distribution data of different coatings under different thickness conditions. The initial temperature of the plasma-sprayed iron-based coating at 0 micrometers is 1930°C. As the thickness increases, the temperature gradually decreases, stabilizing at 1200°C after 1200 micrometers. The initial temperature of the non-coated material is 1880°C, with a faster temperature decrease, reaching 1400°C at 800 micrometers and stabilizing at 1260°C after 1200 micrometers. The initial temperature of the tungsten-cobalt alloy coating (single layer) is 1840°C, decreasing to 1240°C after 1000 micrometers and remaining constant. The tungsten-cobalt alloy coating (double layer) has the lowest initial temperature of 1800°C, decreasing to 1320°C at 800 micrometers and stabilizing at 1300°C after 1000 micrometers. The data analysis shows significant differences in thermal conductivity performance among different coatings. The plasma-sprayed iron-based coating shows a gentle temperature decrease as the thickness increases, stabilizing at 1200°C after 1200 micrometers, demonstrating good thermal insulation and temperature stability. The non-coated material has the fastest temperature decrease, indicating the poorest thermal insulation effect and weaker thermal conductivity. The tungsten-cobalt alloy coatings (single and double layers) exhibit good thermal conductivity, with the double-layer coating stabilizing at 1300°C after 1000 micrometers, which is higher than the single-layer coating but still better than the non-coated material.

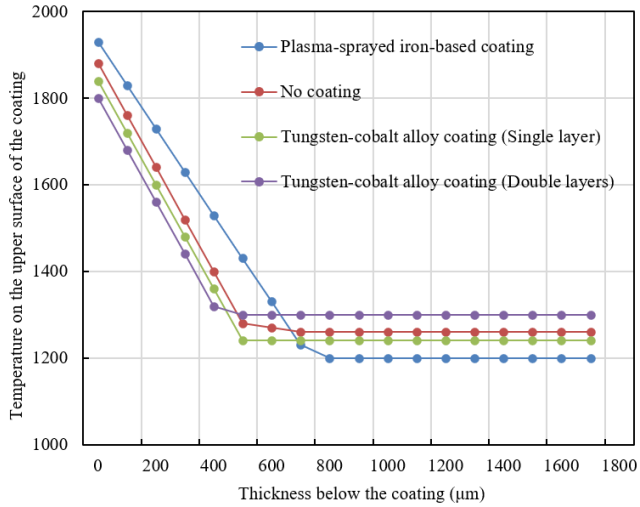

Figure 6. Temperature distribution within different coatings

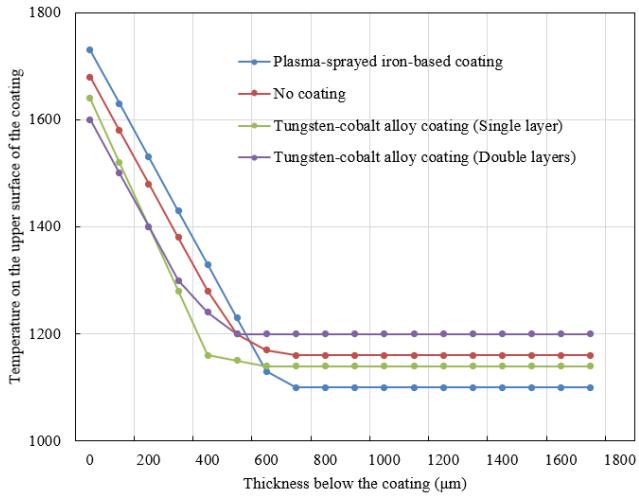

Figure 7. Temperature distribution within different coatings under the assumption of no radiative heat transfer

Figure 7 shows the temperature distribution data of different coatings under different thickness conditions. For the plasma-sprayed iron-based coating, the initial temperature is 1730°C, and as the thickness increases, the temperature gradually decreases, stabilizing at 1100°C after 1200 micrometers. The initial temperature of the non-coated material is 1680°C, with a faster temperature decrease, reaching 1200°C at 1000 micrometers and stabilizing at 1160°C after 1200 micrometers. The initial temperature of the tungsten-cobalt alloy coating (single layer) is 1640°C, decreasing to 1140°C after 1000 micrometers and remaining constant. The tungsten-cobalt alloy coating (double layers) has the lowest initial temperature of 1600°C, decreasing to 1200°C at 1000 micrometers and stabilizing at 1200°C after 1200 micrometers. Data analysis shows significant differences in the thermal conductivity performance of different coatings under the assumption of no radiative heat transfer. The plasma-sprayed iron-based coating shows a gentle temperature decrease as the thickness increases, stabilizing at 1100°C, demonstrating good thermal insulation and temperature stability. The non-coated material has the fastest temperature decrease, indicating the poorest thermal insulation effect and weaker thermal conductivity. The tungsten-cobalt alloy coatings (single and double layers) stabilize at 1140°C and 1200°C, respectively, after 1000 micrometers, showing better thermal insulation than the non-

coated material.

This paper established a coupled heat transfer model for plasma-sprayed iron-based coatings, accurately calculating the thermal conductivity performance of the coating under different working conditions and validating the model's effectiveness with experimental data. This study not only confirmed the excellent performance of plasma-sprayed iron-based coatings in high-temperature environments but also provides important theoretical support and practical references for optimized design and thermal management in practical applications.

5. CONCLUSION

This paper established a coupled heat transfer model for plasma-sprayed iron-based coatings, deeply exploring the thermal conductivity performance of the coating under different working conditions. The research mainly includes three parts: first, the theoretical analysis established the mathematical derivation of the coupled heat transfer model within the plasma-sprayed iron-based coating, ensuring the model's precision; second, the determination of conductive boundary conditions and calculation of heat transfer coefficients for the plasma-sprayed iron-based coating, ensuring the model's accuracy and applicability; finally, the numerical simulation methods validated the model's effectiveness, demonstrating the excellent thermal conductivity characteristics of plasma-sprayed iron-based coatings in high-temperature environments.

Experimental results show significant differences in the thermal conductivity performance of the coatings under different conditions. By comparing the temperature variations of different coatings at room temperature, the surface temperature changes with load, and the extremely low maximum stress changes over time, it can be seen that the plasma-sprayed iron-based coating shows a gentle temperature decrease as the thickness increases, demonstrating good thermal insulation and temperature stability. Especially under the assumption of no radiative heat transfer, the temperature distribution of the plasma-sprayed iron-based coating is more uniform, further validating the model's accuracy and effectiveness. These results not only confirm the excellent performance of plasma-sprayed iron-based coatings in high-temperature environments but also provide important theoretical basis and practical guidance for optimized design and thermal management in industrial applications.

This study has achieved important results in analyzing the thermal conductivity performance of plasma-sprayed iron-based coatings, providing accurate mathematical models and validation data, and offering theoretical support for optimized coating design in industrial applications. However, this study also has some limitations. First, the research mainly focuses on the thermal conductivity performance of plasma-sprayed iron-based coatings and does not deeply explore the performance of other types of coatings and under different environmental conditions. Second, the experimental data is primarily based on numerical simulations, which might be influenced by other factors in actual applications, such as environmental humidity and mechanical stress. Future research can further extend to the analysis of thermal conductivity performance of other types of coatings and combine experimental data under actual industrial environments for validation. Additionally, exploring the performance of coatings under different environmental conditions (such as high humidity and strong mechanical stress) can provide guidance for coating materials in broader application fields. These studies will help improve the reliability and performance of coating materials in practical applications and promote the development of related technologies.

ACKNOWLEDGEMENTS

This paper was supported by Scientific Research Project of Ningxia Education Department, Outstanding Young Teacher Support Program, “Research on Repairing the Cathode Tube of Industrial Sodium Electrolytic Cell by Laser Cladding Technology”.

REFERENCES

[1] Bao, F., Yamashita, S., Daki, H., Nakagawa, K., Kita, H. (2024). Microstructure modification of alumina prepared by water-stabilized plasma spraying method using Al-Cu-O reaction. Journal of the European Ceramic Society, 44(10): 6113-6123. https://doi.org/10.1016/j.jeurceramsoc.2024.03.016

[2] Huang, Q., Chen, S., Liu, M., Zhou, X., Huang, Y., Wang, H. (2023). Research status of reactive plasma spraying technology. Cailiao Daobao/Materials Reports, 37(20): 66-77. https://doi.org/10.11896/cldb.22030146

[3] Srividya, K., Reddy, S.P., Prasad, K.H., Thati, N.S.R.K., Snehita, K., Pranay, U.S., Yellapragada, N.V.S. (2023). Optimization of process parameters for preparation of Lanthanum Hexa-Aluminate powders using combinatorial approach of Taguchi-GRA and ACO methods. Annales de Chimie - Science des Matériaux, 47(1): 43-50. https://doi.org/10.18280/acsm.470106

[4] Al-Ubaidy, S.K., Bouraoui, C. (2024). High-entropy alloys: Advantages and applications in challenging environments. Annales de Chimie - Science des Matériaux, 48(1): 125-136. https://doi.org/10.18280/acsm.480115

[5] Yang, G., Fu, B., Dong, T., Li, G. (2024). Preparation of AlSi30Cu5 coating with fine microstructure using plasma spraying technology. Materials Letters, 357.

[6] Zhang, Y., Lv, Y., Yuan, Y., Tang, S., Liu, T., Fan, J. (2024). Effect of suspension plasma spraying power on the microstructure and properties of Cr2AlC coatings. Applied Surface Science, 648: 159034. https://doi.org/10.1016/j.apsusc.2023.159034

[7] Sun, W.W., Yang, Y., Wang, Y.W. (2024). High entropy carbide (ZrNbTiCr) C ceramic composite coating with fine grains fabricated by plasma spraying. Surface and Coatings Technology, 478: 130459. https://doi.org/10.1016/j.surfcoat.2024.130459

[8] St Węglowski, M., Śliwiński, P., Dymek, S., Kalemba-Rec, I., Kapuściński, M., Wrona, A., Kustra, K. (2023). A comprehensive study on the microstructure of plasma spraying coatings after electron beam remelting. In Journal of Physics: Conference Series, Varna, Bulgaria, p. 012005. https://doi.org/10.1088/1742-6596/2443/1/012005

[9] Niu, X., Huang, P., Wang, Y., Zou, B. (2023). Preparation and characterization of a composite ceramic

coating containing absorber LaFe12O19 by plasma spraying. Ceramics International, 49(16): 27079-27085. https://doi.org/10.1016/j.ceramint.2023.05.252

[10] Lei, S., Huang, Y., Liu, M., Zhao, Y., Wang, H. (2023). Microstructure and corrosion resistance of iron-based amorphous coatings sprayed by plasma transfer arc. Cailiao Gongcheng/Journal of Materials Engineering, 51(10): 107-117. https://doi.org/10.11868/j.issn.1001-4381.2022.000042

[11] Pathak, A., Mukherjee, B., Pandey, K.K., Islam, A., Bijalwan, P., Dutta, M., Keshri, A.K. (2022). Process—structure—property relationship for plasma-sprayed iron-based amorphous/crystalline composite coatings. International Journal of Minerals, Metallurgy and Materials, 29: 144-152. https://doi.org/10.1007/s12613-020-2171-4

[12] Małachowska, A., Sokołowski, P., Paczkowski, G., Lampke, T., Sajbura, A. (2022). Comparison of microstructures and selected properties of plasma-sprayed iron-based metallic glass coatings. Journal of Thermal Spray Technology, 31(4): 1330-1341. https://doi.org/10.1007/s11666-022-01355-7

[13] Zhou, Z., Zhang, L., Dong, X., Luo, X., Mahrukh, M., Li, C. (2023). Mechanism of suppressing oxidation of FeAl molten droplet by adding c to powder and its effect on microstructure and properties of plasma-sprayed coating. Zhongguo Biaomian Gongcheng/China Surface Engineering, 36(1): 44-56. https://doi.org/10.11933/j.issn.1007-9289.20220506004

[14] Li, Y., Meng, Z., Chen, Y., Shen, J., Li, Y., Zhou, Y., Zhang, X. (2024). Effect of La2O3 on hardness, wear resistance and corrosion resistance of WC/Fe90 iron-based composite coatings. Journal of Alloys and Compounds, 992: 174584. https://doi.org/10.1016/j.jallcom.2024.174584

[15] Gao, R., Huang, Y., Zhou, X., Ma, G., Jin, G., Li, T., Wang, H., Liu, M. (2024). Material system and tribological mechanism of plasma sprayed wear resistant coatings: Overview. Surface and Coatings Technology, 483: 130758. https://doi.org/10.1016/j.surfcoat.2024.130758

[16] Li, C., Dai, H., Zhong, Y. (2020). Analytical solutions for fourier and non-fourier heat conduction in thermal barrier coating of efficient engine. Journal of the Chinese Society of Mechanical Engineers, Transactions of the Chinese Institute of Engineers, Series C/Chung-Kuo Chi Hsueh Kung Ch'eng Hsuebo Pao, 41(2): 181-188.

[17] Shevchuk, V.A., Gavris', A.P. (2020). Nonstationary heat-conduction problem for a half-space with a multilayer coating upon cyclic change in the ambient temperature. Journal of Engineering Physics and Thermophysics, 93(6): 1489-1497. https://doi.org/10.1007/s10891-020-02254-w

[18] Kulchytsky-Zhyhailo, R., Matysiak, S.J., Perkowski, D.M. (2020). On the quasi-stationary problem of heat conduction for a homogeneous half-space with composite coating. Acta Mechanica, 231(3): 1241-1251. https://doi.org/10.1007/s00707-019-02591-9

[19] Lu, R., Xu, F., Cui, Y., Bao, D., Yuan, S., Sun, Y., Wang, H. (2024). Novel thermal conductivity and anti-corrosion coating with hydrophobic properties for heat exchanger applications. Progress in Organic Coatings, 186: 108004. https://doi.org/10.1016/j.porgcoat.2023.108004

[20] Jasiewicz, E., Hadała, B., Kubaszek, T., Kościelniak, B., Cebo-Rudnicka, A., Dychtoń, K., Pędrak, P. (2024). The influence of MCrAlY coating application and its thickness on the heat transfer during water spray cooling. International Journal of Heat and Mass Transfer, 220: 124985. https://doi.org/10.1016/j.ijheatmasstransfer.2023.124985

[21] Shi, S., Zhang, Y., Hu, L., Fang, G., Cui, X. (2023). Ablation mechanism and coupling pyrolysis/conduction model of a silicone rubber matrix thermal protection coating. Hangkong Dongli Xuebao/Journal of Aerospace Power, 38(9): 2049-2061. https://doi.org/10.13224/j.cnki.jasp.20220897

[22] Formalev, V.F., Degtyarenko, R.A., Garibyan, B.A., Kolesnik, S.A. (2022). Modeling heat and mass transfer during periodical spraying of a high-temperature heat-resistant coating. High Temperature, 60: S76-S80. https://doi.org/10.1134/S0018151X21040106